

Peripapillary Sparing With Near Infrared Autofluorescence Correlates With Electroretinographic Findings in Patients With Stargardt Disease

Marco Nassisi,¹ Saddek Mohand-Saïd,² Camille Andrieu,² Aline Antonio,¹ Christel Condroyer,¹ Cécile Méjécasse,¹ Claire-Marie Dhaenens,³ José-Alain Sahel,^{1,2,4-6} Christina Zeitz,¹ and Isabelle Audo^{1,2,7}

¹Sorbonne Université, Institut National de la Santé et de la Recherche Médicale, Centre National de la Recherche Scientifique, Institut de la Vision, Paris, France

²Centre Hospitalier National d'Ophthalmologie des Quinze-Vingts, DHU Sight Restore, INSERM-DHOS CIC 1423, Paris, France

³University of Lille, Institut National de la Santé et de la Recherche Médicale UMR-S 1172, CHU Lille, Biochemistry and Molecular Biology Department-UF Génopathies, Lille, France

⁴Fondation Ophthalmologique Adolphe de Rothschild, Paris, France

⁵Académie des Sciences-Institut de France, Paris, France

⁶Department of Ophthalmology, The University of Pittsburgh School of Medicine, Pittsburg, Pennsylvania, United States

⁷Institute of Ophthalmology, University College of London, London, United Kingdom

Correspondence: Isabelle Audo, Institut de la Vision, 17 Rue Moreau, Paris, France, 75012; isabelle.audo@inserm.fr

Submitted: March 14, 2019
Accepted: October 2, 2019

Citation: Nassisi M, Mohand-Saïd S, Andrieu C, et al. Peripapillary sparing with near infrared autofluorescence correlates with electroretinographic findings in patients with Stargardt disease. *Invest Ophthalmol Vis Sci*. 2019;60:4951-4957. <https://doi.org/10.1167/iovs.19-27100>

PURPOSE. To evaluate the correlation between the quantification of peripapillary sparing and electroretinogram (ERG) outcomes in autosomal recessive Stargardt disease (STGD1).

METHODS. Near infrared fundus autofluorescence (NIR-FAF) images of 101 eyes of 101 patients were retrospectively reviewed. Peripapillary sparing was assessed both qualitatively and quantitatively. The area of spared tissue (AST) was calculated in a 1-mm-wide ring around the optic disc after binarization of the 55° NIR-FAF. These measurements were correlated with the presence of normal ERG (group I), abnormal photopic responses (group II), or abnormal photopic and scotopic responses (group III).

RESULTS. AST showed significant correlations with ERG groups ($R = -0.802$, $P < 0.001$). While qualitative assessment of peripapillary sparing (i.e., present or not) also showed a significant correlation with ERG groups ($R = -0.435$, $P < 0.001$), it was weaker than by AST quantification. The ordinal regression analysis showed that the increase in AST was associated with a decrease in the odds of belonging to ERG groups II and III, with an odds ratio of 0.82 (95% confidence interval [CI] 0.78-0.87), $P < 0.001$.

CONCLUSIONS. The AST around the optic disc in eyes with STGD1 correlates with the impairment of photoreceptors as shown in the ERG. If replicated in future longitudinal studies, the quantification of peripapillary sparing may prove to be a useful parameter for evaluating the visual prognosis of these eyes.

Keywords: Stargardt disease, near infrared autofluorescence, peripapillary sparing, electrophysiology

Autosomal recessive Stargardt disease (STGD1) (MIM# 248200) is the most common form of inherited macular degeneration both in children and young adults, characterized by progressive loss of central vision.¹ It is caused by mutations in the ATP-binding cassette transporter 4 (*ABCA4*) gene (MIM# 601691).² Although genetically well characterized, STGD1 is phenotypically heterogeneous with a range of manifestations that could go from an early-onset central atrophy to a late-onset disease with foveal sparing, to a maculopathy or a more generalized disease leading to cone-rod dystrophy, therefore associated with very different prognosis and visual ability expectancy.¹ A functional classification, based on full-field electroretinogram (ERG) (ff-ERG) results, reflects this variability in visual prognosis.³ Briefly, group I is characterized by normal ff-ERG, while group II shows abnormal photopic responses and group III has both cone and rod responses impaired. Of course,

the difference between these groups is in the prognosis, with groups II and III leading to an earlier and more severe visual impairment. One of the features of *ABCA4*-related disease is a relative peripapillary sparing, characterized by the absence of flecks and retinal pigment epithelium (RPE) atrophy in the peripapillary region of the retina.⁴⁻⁶ The presence of atrophy in the peripapillary area is reported in non-group I STGD1.^{7,8} Given these findings, it has been suggested that the peripapillary area could be a region of interest for monitoring the efficacy of treatment in this disease.^{5,8} The integrity of the peripapillary area can be assessed by using fundus autofluorescence.^{9,10} In STGD1, near infrared fundus autofluorescence (NIR-FAF) can reveal areas of decreased autofluorescence (or hypoaufluorescence [hypoAF]) that correlate with regions of photoreceptor damage, that is, areas of ellipsoid zone (EZ) band loss on optical coherence tomography (OCT) (Fig. 1).¹⁰ A



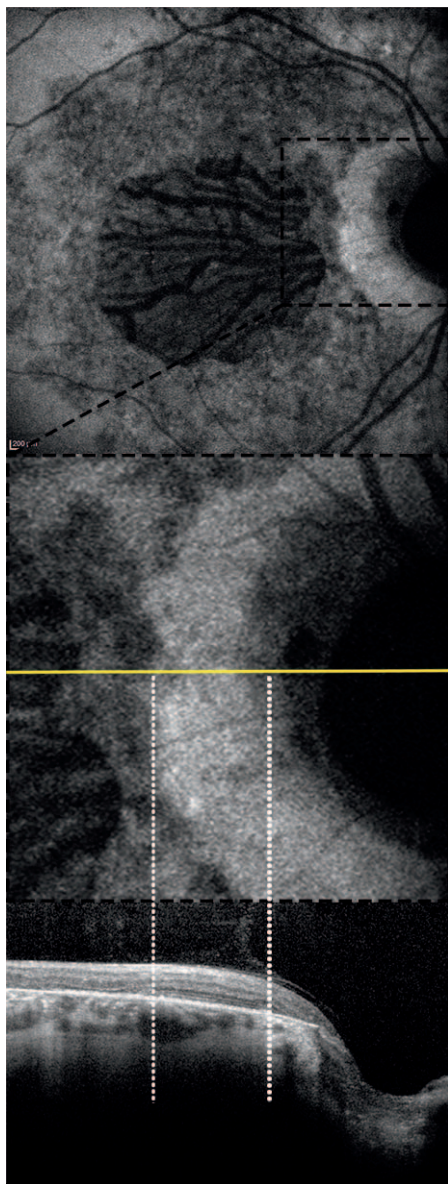


FIGURE 1. A 30° near infrared fundus autofluorescence of a patient with STGD1 is shown on *top*. The peripapillary area (highlighted in the *black box* and enlarged in the *middle*) was correlated with an SD-OCT B-scan (*bottom*), passing through the *yellow line*. The limits of the near infrared hypoautofluorescent area (*white dotted lines*) correspond to the area of preservation of both retinal pigment epithelium and ellipsoid zone band on SD-OCT.

qualitative assessment of the peripapillary sparing is not always straightforward, and whether quantification of the spared tissue around the optic disc could improve the accuracy of the ERG group prediction has never been tested. The aim of this study was to retrospectively review the NIR-FAF of patients with STGD1 and develop a semiautomated method to quantify the peripapillary sparing. We then evaluated the correlation between this sign and the ERG groups.

METHODS

In this retrospective analysis, we collected and analyzed the charts, the NIR-FAF images, and the ERGs of consecutive patients with clinical and molecular diagnosis of STGD1

disease, acquired at the Reference Center for rare diseases, Referet, of the Quinze-Vingts hospital in Paris between January 2016 and August 2018. Most of the molecular analyses were performed at the Institut de la Vision, Sorbonne Université, Institut National de la Santé et de la Recherche Médicale (INSERM), with a combination of microarray analysis and Sanger sequencing of *ABCA4* as previously reported.¹¹ Evidence of any other pathology involving the macula and/or the optic nerve was an exclusion criterion in this study.

The 55° of field NIR-FAF images (Heidelberg Retina Angiograph [HRA II], 787-nm excitation; Heidelberg Engineering, Heidelberg, Germany) were retrospectively reviewed and evaluated for quality and resolution. Main criteria for image inclusion were as follows: (1) The image was the result of at least 30 averaged frames; (2) the image was centered on the fovea, on the optic nerve, or on the space between them; (3) there was a clear demarcation between the damaged and the spared tissue. When images from both eyes could be included in the study, the right eye was chosen for analysis. The NIR-FAF images of the right eyes of 20 healthy volunteers were also included in the study as controls. All eligible patients required the electrophysiological assessment done on the same day as image acquisition. Full-field ERG was recorded on a Diagnosys Espion system with the ColorDome LED full-field stimulator (Diagnosys LLC, Lowell, MA, USA). The stimulation protocol incorporated the minimum standards of the International Society for Clinical Electrophysiology of Vision (ISCEV).¹² In brief, after 20 minutes of dark adaptation, responses to the following flash intensities were recorded: 0.01, 3, and 10 cd.s/m². This was followed by 8 minutes of light adaptation, and responses to a 2-Hz and a 30-Hz flicker of 3.0 cd.s/m² were recorded. The patient data sets were compared against those of 30 healthy subjects (Supplementary Table S1). The limits of ERG normality for both implicit time and amplitude were defined for all the components of the ERG as the mean value \pm 2 standard deviations. All the components of the ERG from each eye were taken into account when classifying patients into the three ERG groups defined by Lois et al.³ In particular, photopic responses were considered abnormal when implicit times were delayed and amplitudes were reduced to both 2- and 30-Hz stimuli. Scotopic responses were considered abnormal when implicit times were delayed and amplitudes were reduced to all stimuli. The study protocol adhered to the tenets of the Declaration of Helsinki and was approved by the local ethics committees.

Image Analysis

The peripapillary sparing in NIR-FAF images was analyzed both qualitatively (present or not) and quantitatively.

For the qualitative assessment, the peripapillary area was considered preserved when a uniform annulus of NIR autofluorescence was present and no areas of hypoAF were observed within an eccentricity of 0.6 mm from the optic disc.⁸

For the quantification of the spared tissue, all images were imported in ImageJ (version 1.50; National Institutes of Health, Bethesda, MD, USA; <http://rsb.info.nih.gov/ij/index.html>; in the public domain).¹³

First, the edge of the optic disc was outlined; then, using the “distance map” function, a concentric 1-mm-wide ring was obtained. A Gaussian blur filter (radius 1) was applied to despeckle the image; then, after the binarization of the image using an automatic local thresholding method (MidGrey, radius = 30 pixels), the area of spared tissue (AST) was calculated as percentage of the ring area, using the “Analyze particles” command (size: 0-infinity, circularity 0-1) (Fig. 2). All NIR-FAF analyses were performed by two trained independent opera-

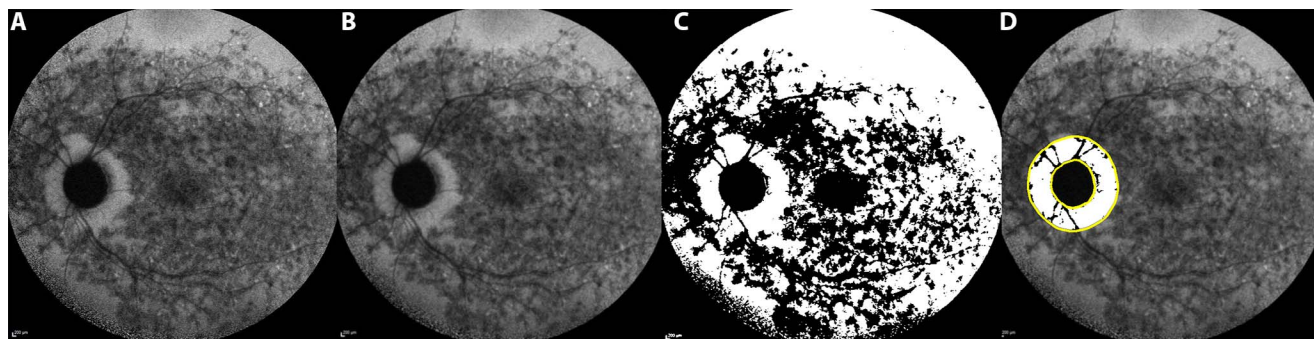


FIGURE 2. A 55° near infrared fundus autofluorescence image was used for the quantification of the spared tissue in the peripapillary area (A). After the application of a gaussian blur filter (B) a threshold was applied to binarize the image (C) and to measure the area of spared tissue (white pixels) within a 1-mm-wide ring outside the optic disc (yellow lines, D).

tors (M.N., I.A.). The first grader reviewed all cases; the second grader independently reviewed a randomly selected sample of 40 study eyes to assess the intergrader repeatability. Any case of disagreement in the qualitative assessment was evaluated by open adjudication. If no consensus was reached, a final decision was made by the medical director of the unit (J.-A.S.).

Statistical Analysis

Kruskal-Wallis and Mann-Whitney *U* tests were used to compare the ERG groups for continuous variables while χ^2 test was used for categorical variables. The correlations between qualitative or quantitative assessment of peripapillary sparing and ERG groups were analyzed using Spearman’s ρ test. The same test was used to correlate age of onset (defined as the age when the patient first noted visual symptoms) and duration of the disease (defined as the difference between age at the time of the examination and age of onset) with AST. Comparisons between significant correlations were made with Fisher’s *r* to *z* transformation and then by comparing the *z* scores for statistical significance by determining the observed *z* test statistic. The association between peripapillary involvement in the qualitative assessment or AST and ERG groups was further investigated with an ordinal regression analysis. Nonparametric receiver operating characteristic (ROC) curves were generated for AST and the distinction between ERG group 1 vs. 2 and between ERG group 2 vs. 3. Prediction accuracy of AST was determined by calculating the area under the curve (AUC) for each ROC curve. The intraclass correlation coefficient (ICC) was calculated to test the repeatability of the quantitative method. A linear regression analysis was performed to investigate the association between AST and genotype. All data are presented as mean \pm standard deviation. A *P* value < 0.05 was considered significant in this analysis.

TABLE. Demographic Data of the Subjects Included in the Study. A χ^2 Test Was Performed for Sex, While a Kruskal-Wallis Test Was Performed for Age at Examination and Age of Onset

Groups	Sex, Female/Total	Age of Onset, Mean \pm SD, Years	Age at Examination, Mean \pm SD, Years
ERG group I	30/42	24 \pm 13.5	30.1 \pm 14.9
ERG group II	19/40	22.9 \pm 13.6	29.6 \pm 16.2
ERG group III	5/19	15.9 \pm 9.5	30.2 \pm 18.6
<i>P</i> value	0.003	0.029	0.929

RESULTS

A total of 101 eyes from 101 patients with molecular diagnosis of STGD1 disease were eligible for image analysis (Fig. 3). All genotypic information is reported in Supplementary Table S2. Forty-two patients had normal ff-ERG (group I), 40 had altered photopic responses (group II), and 19 had both photopic and scotopic responses impaired (group III). Demographic data for each group are reported in the Table. The three groups differed significantly for the age of onset and sex distribution but not for the age at examination. Peripapillary sparing was present in 32/42, 20/40, and 3/19 in group I, II, and III, respectively (*P* < 0.001). A post hoc analysis performed applying a Bonferroni correction for three pairwise comparisons (significant *P* value < 0.017) revealed a significant difference in the distribution of the peripapillary sparing between all the ERG groups (*P* < 0.001 for groups I and III, *P* = 0.014 for groups I and II, and *P* = 0.012 for groups II and III). The Spearman correlation coefficient (*R*) was -0.435 (*P* < 0.001). The presence of peripapillary sparing reduces the risk of belonging to ERG group II or III, with an odds ratio of 0.17 (95% confidence interval [CI] 0.07–0.38, *P* < 0.001).

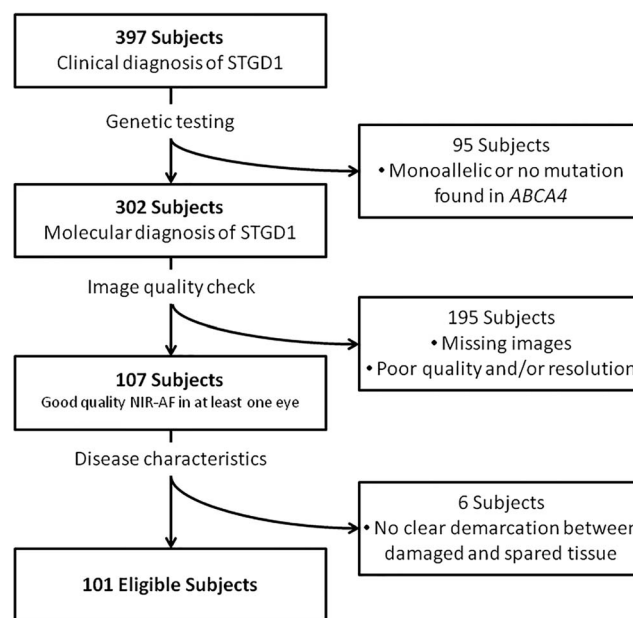


FIGURE 3. Flow chart diagram explaining the selection process of eligible eyes for this study.

Group I had an AST of $83.9 \pm 8.8\%$, which was not significantly different from the control group ($85.7 \pm 3.4\%$, $P = 0.588$). However, it was different from both group II and group III ($63.8 \pm 10.7\%$, $P < 0.001$ and $46.5 \pm 10.5\%$, $P < 0.001$, respectively). Furthermore, the statistical difference remained significant when comparing groups II and III ($P < 0.001$) (Fig. 4). Correlation between AST and ERG groups was strongly significant ($R = -0.802$, $P < 0.001$) and significantly higher than the qualitative assessment ($P < 0.001$). The ordinal regression analysis showed that the increase in AST was associated with a decrease in the odds of belonging to ERG groups II and III, with an odds ratio of 0.82 (95% CI, 0.78–0.87), $P < 0.001$. No significant correlation was found between age of onset and duration of the disease and AST. With respect to the discrimination between ERG groups 1 and 2, ROC AUC value was 0.93 (standard error [SE]: 0.29; 95% CI: 0.87–0.98). With respect to the discrimination between ERG groups 2 and 3, ROC AUC value was 0.88 (SE: 0.06; 95% CI: 0.77–0.99) (Fig. 5).

Genotype–Phenotype Correlation

The linear regression analysis found no significant associations between the presence of at least one nonsense or frameshift mutation (33 subjects), or the presence of a complex allele (38 subjects) and AST. The allele frequency (AF) of each variant in the cohort is reported in Supplementary Table S2. Only for p.(Gly1961Glu) (AF: 0.09), a significant association was found with AST (coefficient B: 9.13, SE: 4.3, 95% CI: 0.59–17.68, $P = 0.036$).

Repeatability Assessment

The kappa value for intergrader repeatability was 0.9 (36/40) for qualitative assessment of the peripapillary sparing. Agreement was reached for all discrepancies after adjudication between graders. For AST calculation, the ICC was 0.965 (95%CI: 0.931–0.989).

DISCUSSION

Autosomal recessive Stargardt disease is classically characterized by the sparing of the peripapillary retina and RPE even at advanced stages of the disease. A relative eccentricity of approximately 2° (~ 0.6 mm) has been reported as the outer boundary of the spared region. The reasons for this relative sparing in the presence of a widespread disease still remain unclear. Many hypotheses have been advanced to explain this landmark, such as a more favorable photoreceptor/RPE ratio in the peripapillary area, as well as less photo-oxidative damage or lipofuscin accumulation due to a reduced light load on the photoreceptor–RPE complex in the presence of a thicker overlying peripapillary retinal nerve fiber layer (RNFL).^{5,14,15} Burke et al.⁷ proposed this sign as useful for formulating disease severity since its loss was associated with non-group I STGD1 patients, hence with a worse prognosis. All these findings would suggest a potential interest in quantifying the AST around the optic disc, in order to improve the predictability of the disease progression. Overall our results suggest an improvement of the correlation when peripapillary sparing is assessed by quantification. In particular, the strength of the correlation rises to an R value as high as -0.802 for the quantitative assessment. Furthermore, assessing the AST can help in distinguishing between all three ERG groups (Figs. 5, 6). In particular, using the ROC curves, we identified the cutoff values of AST for which the sum of sensitivity and specificity is maximal to discriminate between group 1 vs. 2 (around 75%)

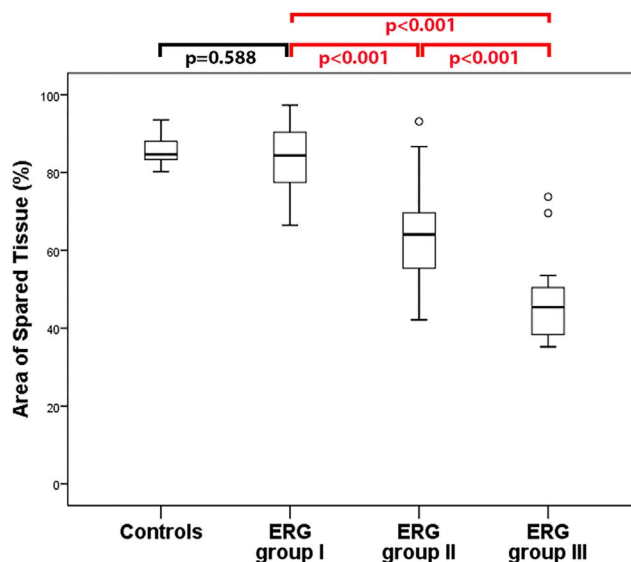
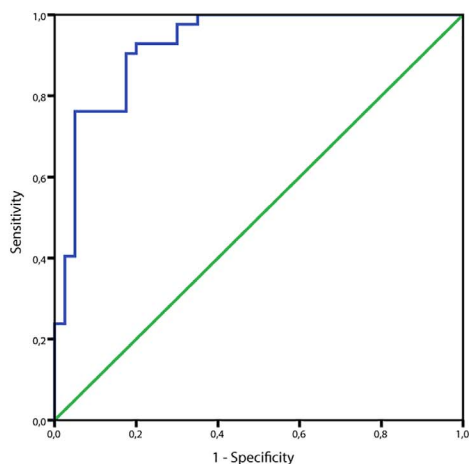


FIGURE 4. Box plot showing the mean values of the areas of spared tissue in each group of patients and controls. The Mann-Whitney U test was performed to test the differences between each group. Significant P values are reported in red.

and group 2 vs. 3 (around 53%). However, it is still debated whether the ERG groups II and III are different entities or are the result of a progressive impairment of the photoreceptors that starts with cones and continues with the involvement of rods. Given the strong correlation between peripapillary sparing and ERG groups, future longitudinal studies including a larger cohort could help to give further insights into this interesting matter. Loss of peripapillary sparing may well be mutation dependent, in that the more severe the mutation in the *ABCA4* gene, the more likely the development of peripapillary atrophy.⁵ In our previous work we demonstrated that among patients carrying at least one null mutation, there is a higher prevalence of peripapillary involvement and photoreceptor impairment (ERG groups II and III).¹¹ In the present study the genotype–phenotype correlation did not reveal any significant association between the presence of a complex allele or of a nonsense or frameshift mutation with the quantification of the peripapillary sparing. These findings might not be surprising considering the variable effect of compound heterozygosity, splicing mutations, or hypomorphic alleles on the function of the *ABCA4* protein.¹⁶ Furthermore, the relatively small cohort and the retrospective nature of our data may have influenced the outcome. No direct association was found between AST and any variant detected in the cohort, except for p.(Gly1961Glu). This mutation is one of the most frequent variants associated with STGD1 (previously reported AF among STGD1 patients: 0.08^{17,18}) and it usually leads to a milder phenotype (i.e., later onset, foveal sparing, normal ERGs).^{17,18} In accordance with these findings, among our cohort, p.(Gly1961Glu) was carried by 19 subjects (AF: 0.09) and its presence was associated with higher values of AST. The most frequent variant detected in our cohort was p.(Asn1868Ile), carried by 25 subjects (AF: 0.12). Despite its high frequency in the general population (Genome Aggregation Database AF:0.04¹⁹), variant p.(Asn1868Ile) has been recently classified as a hypomorphic allele due to its pathogenicity when in trans with “loss-of-function” mutations and its association with a milder STGD1 phenotype.^{20,21} However, we did not find any correlation with AST. When p.(Asn1868Ile) is in cis with other deleterious variants, phenotypes are typically consistent with the effect of the overall genotype with

Group 1 vs Group 2



Group 2 vs Group 3

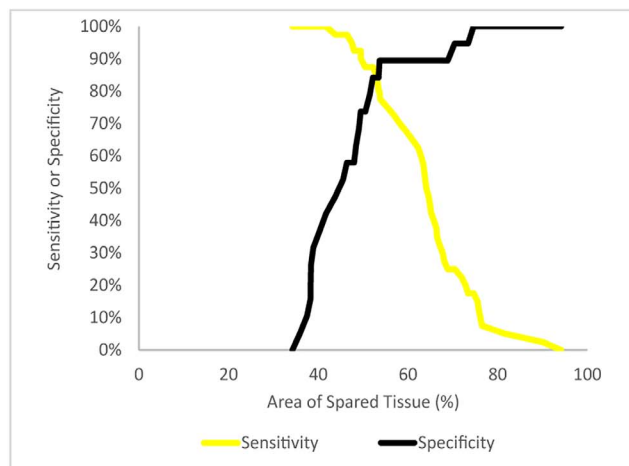
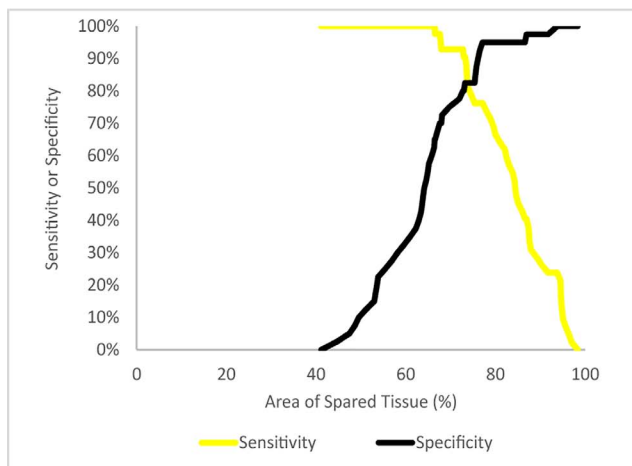
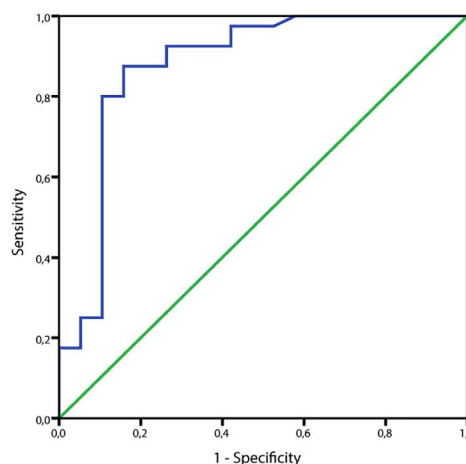


FIGURE 5. Receiver operating characteristic curves for the area of spared tissue for discrimination between ERG groups I and II (*top left*) and between ERG groups II and III (*top right*). An area under the curve of 0.5, corresponding to the diagonal line in each ROC plot, indicates diagnostic accuracy no better than chance, while greater values indicate better diagnostic performance, with a value of 1 being perfect. Sensitivity and specificity plots as a function of AST (*bottom left and right*). The intersection of sensitivity and specificity curves is 74.65% (*bottom left*) for the discrimination between ERG groups I and II. The intersection of sensitivity and specificity curves is 53.24% (*bottom right*) for the discrimination between ERG groups II and III.

mainly early onset and severe disease.^{16,20} In our cohort, 11 subjects carry this variant in cis with other pathogenic mutations while 9 others have more than two *ABCA4* variants (phase determination was impossible due to the absence of family members). Performing a genotype-phenotype correlation using a simplified classification of the variants and/or specific frequent variants is important as it might help clinicians to counsel their patients. However, this may not be as simple in the case of *ABCA4*-related diseases where both mutant alleles may interact specifically with each other. Other methods including the analysis of the proteic domain impacted by the mutation(s), and their effect(s) on the three-dimensional structure of the protein with molecular modeling relationship, might be the next step to understand this complex relationship (Sergeev Y, et al. *IOVS* 2013;54:ARVO E-Abstract 1325).²²

Our study has several limitations that should be considered when assessing our findings. First, since the cohort was collected retrospectively, the study could be subject to

selection bias. Second, we used only NIR-FAF images for assessing the peripapillary sparing. Even though measurements of atrophy are well correlated with measurements from short-wavelength AF (SW-FAF) and OCT, they all may not be measuring the exact same thing.²³⁻²⁵ SW-FAF signal (488-nm excitation) is derived primarily from lipofuscin accumulating in the RPE, while NIR-FAF (787-nm excitation) originates from melanin in the choroid and RPE. In patients with STGD1, both modalities could show areas of hypoAF and areas of hyperautofluorescence (hyperAF) (e.g., flecks and/or rings). However, these abnormal zones can differ in location and extension whether considering SW- or NIR-FAF. In particular, in STGD1, NIR hypoAF is more correlated with the boundary of the EZ band loss and is larger than the SW hypoAF area, which is more roughly correlated to the overall thinning of the outer retinal layers.^{8,10} Thus, the SW-FAF signal can be present in the absence of NIR-FAF, and it can be observed in regions of photoreceptor damage (i.e., in the presence of outer nuclear

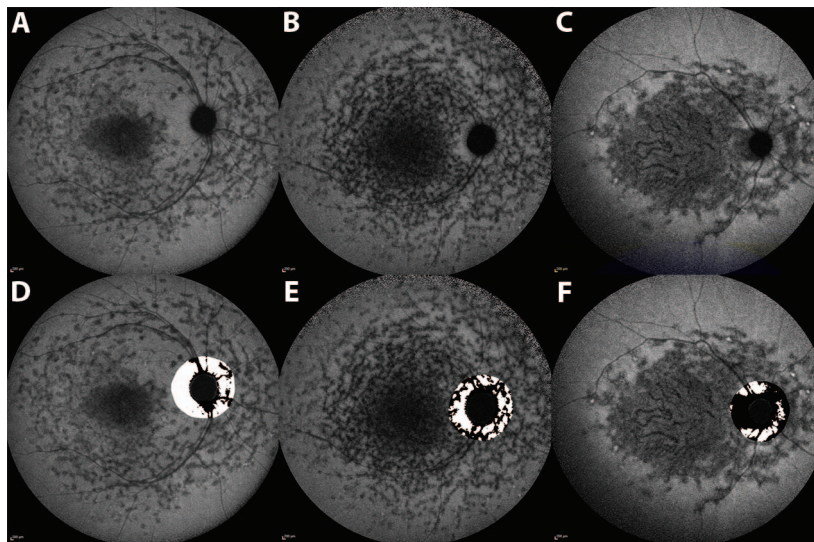


FIGURE 6. Three near infrared fundus autofluorescence images of three patients with STGD1 disease included in the study (A–C) and their respective binarized images (D–F). The first patient (A, D) had normal ff-ERGs and an area of spared tissue of 79.36%; the second patient (B, E) had impaired photopic responses (ERG group II in this study) and had an AST of 59.21%; the third patient (C, F) had both photopic and scotopic responses impaired (ERG group III in this study) and an AST of 41.42%.

layer thinning). Hence, NIR-FAF seems to be more sensitive in predicting the loss of photoreceptors in STGD1. Furthermore, while in SW-FAF flecks can be hyperAF or hypoAF, in NIR-FAF they are predominantly hypoAF.^{9,10} Several hypotheses have been proposed to explain this, including the presence in flecks of lipofuscin-filled swollen RPE cells with apically displaced or reduced melanin^{26,27} or the possibility that while the loss of NIR-FAF signal derives from a loss of RPE cells, the increased SW-FAF signal may derive from photoreceptor outer and inner segments that are degenerating secondary to RPE atrophy.²³ However, regardless of these hypotheses, NIR-FAF displays better-defined alterations with frequent hypoAF lesions; hence the determination of the boundaries of the healthy areas is more reliable, allowing a quantitative assessment of the spared tissue. In our cohort, only six patients were excluded because there was no well-defined demarcation between spared and nonspared tissue around the optic disc; however, this was due to the advanced stage of the disease, with diffuse atrophy all over the posterior pole. Finally, we did not consider the refractive error of the patients as an exclusion criterion. The different axial lengths might have influenced the outcomes of the AST measurements as the 1-mm ring around the optic nerve might not always have the same width. However, all included patients had a refractive error ≤ 3 diopters, and the use of a percentage variable (AST) as the outcome should have limited the impact of axial length on the results of the study.

Nevertheless, our study has also strengths, consisting in the inclusion of only patients with confirmed molecular diagnosis of STGD1 and the use of a semiautomated method to measure the peripapillary sparing on NIR-FAF images. Very good repeatability was achieved using this approach despite the need for manual definition of the optic disc edges. It is worth mentioning that the quantification of peripapillary sparing may be useful not only for STGD1 but also for other diseases in which it is present and can have prognostic value, such as *RDH12*-related Leber congenital amaurosis or *PRPH2*-related inherited retinal diseases.^{5,8,28–30}

In conclusion, our results show that the quantification of peripapillary sparing is correlated with ERG findings in patients with STGD1. If replicated in future longitudinal

studies, this parameter may prove to be useful for evaluating the visual prognosis of these eyes.

Acknowledgments

Supported by Programme Investissements d'Avenir IHU FORE-SIGHT (ANR-18-IAHU-01). The funders had no role in the design and conduct of the study; collection, management, analysis, and interpretation of the data; preparation, review, or approval of the manuscript; and decision to submit the manuscript for publication.

Disclosure: **M. Nassisi**, None; **S. Mohand-Said**, None; **C. Andrieu**, None; **A. Antonio**, None; **C. Condroyer**, None; **C. Méjécasse**, None; **C.-M. Dhaenens**, None; **J.-A. Sahel**, None; **C. Zeitz**, None; **I. Audo**, None

References

1. Tanna P, Strauss RW, Fujinami K, Michaelides M. Stargardt disease: clinical features, molecular genetics, animal models and therapeutic options. *Br J Ophthalmol*. 2017;101:25–30.
2. Allikmets R. A photoreceptor cell-specific ATP-binding transporter gene (ABCR) is mutated in recessive Stargardt macular dystrophy. *Nat Genet*. 1997;17:122.
3. Lois N, Holder GE, Bunce C, Fitzke FW, Bird AC. Phenotypic subtypes of Stargardt macular dystrophy-fundus flavimaculatus. *Arch Ophthalmol*. 2001;119:359–369.
4. Lois N, Halfyard AS, Bird AC, Holder GE, Fitzke FW. Fundus autofluorescence in Stargardt macular dystrophy-fundus flavimaculatus. *Am J Ophthalmol*. 2004;138:55–63.
5. Cideciyan AV, Swider M, Aleman TS, et al. ABCA4-associated retinal degenerations spare structure and function of the human parapapillary retina. *Invest Ophthalmol Vis Sci*. 2005; 46:4739–4746.
6. Hwang JC, Zernant J, Allikmets R, Barile GR, Chang S, Smith RT. Peripapillary atrophy in Stargardt disease. *Retina*. 2009; 29:181–186.
7. Burke TR, Allikmets R, Smith RT, Gouras P, Tsang SH. Loss of peripapillary sparing in non-group I Stargardt disease. *Exp Eye Res*. 2010;91:592–600.
8. Burke TR, Rhee DW, Smith RT, et al. Quantification of peripapillary sparing and macular involvement in Stargardt

- disease (STGD1). *Invest Ophthalmol Vis Sci.* 2011;52:8006–8015.
9. Kellner S, Kellner U, Weber BHF, Fiebig B, Weinitz S, Ruether K. Lipofuscin- and melanin-related fundus autofluorescence in patients with ABCA4-associated retinal dystrophies. *Am J Ophthalmol.* 2009;147:895–902.
 10. Greenstein VC, Schuman AD, Lee W, et al. Near-infrared autofluorescence: its relationship to short-wavelength autofluorescence and optical coherence tomography in recessive stargardt disease. *Invest Ophthalmol Vis Sci.* 2015;56:3226–3234.
 11. Nassisi M, Mohand-Saïd S, Dhaenens C-M, et al. Expanding the mutation spectrum in ABCA4: sixty novel disease causing variants and their associated phenotype in a large French Stargardt cohort. *Int J Mol Sci.* 2018;19:E2196.
 12. McCulloch DL, Marmor MF, Brigell MG, et al. ISCEV Standard for full-field clinical electroretinography (2015 update). *Doc Ophthalmol.* 2015;130:1–12.
 13. Schneider CA, Rasband WS, Eliceiri KW. NIH Image to ImageJ: 25 years of image analysis. *Nat Methods.* 2012;9:671–675.
 14. Sparrow JR, Nakanishi K, Parish CA. The lipofuscin fluorophore A2E mediates blue light-induced damage to retinal pigmented epithelial cells. *Invest Ophthalmol Vis Sci.* 2000;41:1981–1989.
 15. Brandstetter C, Mohr LKM, Latz E, Holz FG, Krohne TU. Light induces NLRP3 inflammasome activation in retinal pigment epithelial cells via lipofuscin-mediated photooxidative damage. *J Mol Med.* 2015;93:905–916.
 16. Zernant J, Lee W, Nagasaki T, et al. Extremely hypomorphic and severe deep intronic variants in the ABCA4 locus result in varying Stargardt disease phenotypes. *Cold Spring Harb Mol Case Stud.* 2018;4:a002733.
 17. Cornelis SS, Bax NM, Zernant J, et al. In silico functional meta-analysis of 5,962 ABCA4 variants in 3,928 retinal dystrophy cases. *Hum Mutat.* 2017;38:400–408.
 18. Fokkema IFAC, Taschner PEM, Schaafsma GCP, Celli J, Laros JFJ, den Dunnen JT. LOVD v.2.0: the next generation in gene variant databases. *Hum Mutat.* 2011;32:557–563.
 19. Lek M, Karczewski KJ, Minikel EV, et al. Analysis of protein-coding genetic variation in 60,706 humans. *Nature.* 2016;536:285–291.
 20. Zernant J, Lee W, Collison FT, et al. Frequent hypomorphic alleles account for a significant fraction of ABCA4 disease and distinguish it from age-related macular degeneration. *J Med Genet.* 2017;54:404–412.
 21. Allikmets R, Zernant J, Lee W. Penetrance of the ABCA4 p.Asn1868Ile allele in Stargardt disease. *Invest Ophthalmol Vis Sci.* 2018;59:5564–5565.
 22. Sergeev YV, Caruso RC, Meltzer MR, Smaoui N, MacDonald IM, Sieving PA. Molecular modeling of retinoschisin with functional analysis of pathogenic mutations from human X-linked retinoschisis. *Hum Mol Genet.* 2010;19:1302–1313.
 23. Sparrow JR, Marsiglia M, Allikmets R, et al. Flecks in recessive Stargardt disease: short-wavelength autofluorescence, near-infrared autofluorescence, and optical coherence tomography. *Invest Ophthalmol Vis Sci.* 2015;56:5029–5039.
 24. Duncker T, Marsiglia M, Lee W, et al. Correlations among near-infrared and short-wavelength autofluorescence and spectral-domain optical coherence tomography in recessive Stargardt disease. *Invest Ophthalmol Vis Sci.* 2014;55:8134–8143.
 25. Greenstein VC, Nunez J, Lee W, et al. A comparison of en face optical coherence tomography and fundus autofluorescence in Stargardt disease. *Invest Ophthalmol Vis Sci.* 2017;58:5227–5236.
 26. Steinmetz RL, Garner A, Maguire JI, Bird AC. Histopathology of incipient fundus flavimaculatus. *Ophthalmology.* 1991;98:953–956.
 27. Eagle RC, Lucier AC, Bernardino VB, Yanoff M. Retinal pigment epithelial abnormalities in fundus flavimaculatus: a light and electron microscopic study. *Ophthalmology.* 1980;87:1189–1200.
 28. Aleman TS, Uyhazi KE, Serrano LW, et al. RDH12 mutations cause a severe retinal degeneration with relatively spared rod function. *Invest Ophthalmol Vis Sci.* 2018;59:5225–5236.
 29. Garg A, Lee W, Sengillo JD, Allikmets R, Garg K, Tsang SH. Peripapillary sparing in RDH12-associated Leber congenital amaurosis. *Ophthalmic Genet.* 2017;38:575–579.
 30. Duncker T, Tsang SH, Woods RL, et al. Quantitative fundus autofluorescence and optical coherence tomography in PRPH2/RDS- and ABCA4-associated disease exhibiting phenotypic overlap. *Invest Ophthalmol Vis Sci.* 2015;56:3159–3170.